Microscopic Origin of Magnetic Anisotropy in Au/Co/Au Probed with X-Ray Magnetic Circular Dichroism

D. Weller,[1] J. Stöhr,[1] R. Nakajima,[2] A. Carl,[1,*] M. G. Samant,[1] C. Chappert,[3] R. Mégy,[3] P. Beauvillain,[3] P. Veillet,[3] and G. A. Held[4]

[1]*IBM Research Division, Almaden Research Center, 650 Harry Road, San Jose, California 95120*
[2]*Materials Science Department, Stanford University, Stanford, California 94305*
[3]*Institut d'Electronique Fondamentale, CNRS UA 22, Université Paris Sud, Bâtiment 220, 91405 Orsay, France*
[4]*IBM Research Division, Thomas J. Watson Research Center, P.O. Box 218, Yorktown Heights, New York 10598*
(Received 1 February 1995)

High-field, angle-dependent x-ray magnetic circular dichroism measurements on a Au/Co-staircase/Au structure reveal an anisotropy in the dichroism intensities parallel and perpendicular to the film plane. The size of this effect is related to the anisotropies of the spin density within the Wigner-Seitz cell and of the orbital magnetic moment, both increasing with decreasing Co thickness. The orbital moment anisotropy is shown to be the microscopic origin of the magnetocrystalline energy anisotropy.

PACS numbers: 78.70.Dm, 78.20.Ls

The microscopic origin of magnetic anisotropy in transition metals is still imperfectly understood. In contrast to ionic compounds where the electrons are confined to each ion [1], the electrons in metals are itinerant and simple magnetic anisotropy pictures based on local bonding or coordination [2] appear to fail [3]. Recently, the interest in this problem has become revived in conjunction with artificially made transition metal films and multilayers with perpendicular magnetic anisotropy (PMA) [4]. It is clear that PMA is due to an intrinsic anisotropy mechanism strong enough to overcome the extrinsic macroscopic shape anisotropy, which favors an in-plane orientation of the magnetization. It can generally be viewed as arising from anisotropies in the crystalline lattice, i.e., from (a generalized) magnetocrystalline anisotropy (MCA), including such effects as symmetry breaking and strain. One usually distinguishes contributions from surfaces (interface anisotropy) [2] and from the bulk crystal lattice (volume anisotropy) [5,6]. In the past, experimental studies have mainly concentrated on characterizing MCA through the measurement of the various phenomenological anisotropy energy constants [4,6], which can be compared with those obtained from electronic structure calculations [3,7–13]. Owing to the small values of these energies (10^{-3}–10^{-7} eV/atom) the reliable prediction of MCA is still a challenge for the most advanced theoretical methods. Even if successful, physical insight is often lost because of the complexity of the calculations.

The present paper provides direct experimental support for a simple picture for the microscopic origin of the MCA, which quantitatively relates energy anisotropy to orbital moment anisotropy [5,14]. Using high-field angle-dependent x-ray magnetic circular dichroism (XMCD) spectroscopy we show that the perpendicular orientation of the magnetization direction in Au/Co/Au sandwiches is a consequence of a large anisotropy of the Co orbital magnetic moment. With decreasing Co film thickness the orbital moment becomes increasingly anisotropic, with a larger value perpendicular to the film [15]. The perpendicular orientation of the total moment is due to the orbital moment that redirects the spin moment into a perpendicular alignment through spin-orbit coupling, thus overcoming the in-plane shape anisotropy due to the spin-spin dipole interaction. Our measurements furthermore reveal an anisotropy in the spin density within the atomic sphere, as predicted recently [14]. Both effects have a common microscopic origin: the anisotropy of the lattice [14].

The Au/Co-staircase/Au sample was made by room temperature deposition of the metals in ultrahigh vacuum, with background pressures below 5×10^{-10} mbar during film growth [18]. First a 28 nm thick Au buffer is grown onto a float-glass substrate, which after annealing for 1 h at 175 °C provides an atomically flat and fully (111) textured template. Subsequently, ten Co terraces of 2 mm width and thicknesses between 3 and 12 atomic layers (AL's) of Co are generated at the low growth rate of 0.3 AL/min using a linear shutter, and are finally capped with an ≈9 AL thick Au layer. The Co staircase sample was characterized by angle-dependent polar Kerr hysteresis measurements in fields up to 20 kOe [17]. Plateaus in both the coercivity and the Kerr rotation confirmed its steplike structure [18]. The intrinsic energy anisotropy (per Co volume), K_1, was found to follow a typical $K_V + 2K_S/t_{\mathrm{Co}}$ dependence with volume and surface anisotropy constants $K_V = 0.45$ MJ/m^3 and $K_S = 0.73$ MJ/m^2, respectively. The size of K_V together with the observation of second order anisotropy constants $K_2 = 0.1$–0.2 MJ/m^3 are consistent with mostly hexagonal (0001) Co. The transition from out-of-plane to in-plane anisotropy occurs at $t^* \approx 11$ AL [19].

XMCD measurements were performed at room temperature at the Stanford Synchrotron Radiation Laboratory (SSRL) on beamline 8-2 as discussed previously [16].

 0031-9007/95/75(20)/3752(4)$06.00

Spectra were recorded in a 10 kOe external magnetic field parallel to the x-ray propagation direction, at angles $\gamma = 0°$ and 65° with respect to the surface normal. X-ray absorption was measured by the photocurrent from the sample using right circularly polarized x rays and switching the magnetization direction parallel and then antiparallel to the photon spin at each photon energy step. A cylindrically symmetric electric bias field of +200 V was used to collect the photogenerated electrons from the grounded sample. This avoids experimental asymmetries in the presence of large magnetic fields. The spectra were flux normalized and, after subtraction of a linear background, were scaled to the same edge jump in the region above 820 eV. This ensures that the measured dichroism signal corresponds to a per atom basis. Measurements for different Co thicknesses were performed by translating the sample along the wedge direction. The x-ray beam spot size was about 0.75 mm along the translation direction, assuring adequate spatial resolution.

Normalized Co $L_{2,3}$ XMCD difference spectra for two Co steps at normal and grazing x-ray incidence are shown in Fig. 1. Spin (m_{spin}) and orbital (m_{orb}) Co d moments were determined from the L_3 and L_2 dichroism intensities, denoted ΔA_{L_3} and ΔA_{L_2}, respectively. We used the dichroism sum rules [20–23] together with the renormalization method of Samant *et al.* [24]. The angle-dependent orbital moment $m_{\mathrm{orb}}^{\gamma} = -\langle L_z \rangle_{\gamma} \mu_B/\hbar$ can be determined from [14,20],

$$[\Delta A_{L_3} + \Delta A_{L_2}]_{\gamma} = -\frac{C}{2\mu_B} m_{\mathrm{orb}}^{\gamma}, \qquad (1)$$

where γ indicates the x-ray incidence angle from the surface normal [25]. In hexagonal Co, in-plane anisotropies can be neglected, and we denote normal and in-plane components as $m_{\mathrm{orb}}^{\perp} = m_{\mathrm{orb}}^{z}$ and $m_{\mathrm{orb}}^{\parallel} = m_{\mathrm{orb}}^{x,y}$, respectively. The spin moment $m_{\mathrm{spin}} = -2\langle S_z \rangle \mu_B/\hbar$ is contained in the spin sum rule [14,21]

$$[\Delta A_{L_3} - 2\Delta A_{L_2}]_{\gamma} = -\frac{C}{3\mu_B} (m_{\mathrm{spin}} - 7m_T^{\gamma}), \qquad (2)$$

where $m_T^{\gamma} = \langle T_{\gamma} \rangle \mu_B/\hbar$ is the appropriate component of the d electron expectation value of the intra-atomic magnetic dipole operator $\mathbf{T} = \mathbf{s} - 3\hat{\mathbf{r}}(\hat{\mathbf{r}} \cdot \mathbf{s})$ [21]. $\langle T_{\gamma} \rangle$ reflects the anisotropy of the electron spin density within the Wigner-Seitz cell [14]. The constant C in Eqs. (1) and (2) is proportional to the square of the radial $2p \rightarrow 3d$ transition matrix element and is experimentally determined from the angle averaged dichroism intensities and the known orbital and spin Co d moments, $0.14\mu_B$ and $1.64\mu_B$, respectively [24,26]. The moments $m_{\mathrm{spin}} - 7m_T^{\gamma}$ and $m_{\mathrm{orb}}^{\gamma}$ deduced from the sum rules and corrected for incomplete magnetic saturation are plotted in Figs 2(a) and 2(b), respectively. Using the angle definitions shown in Fig. 2(c) the data correction involved division by

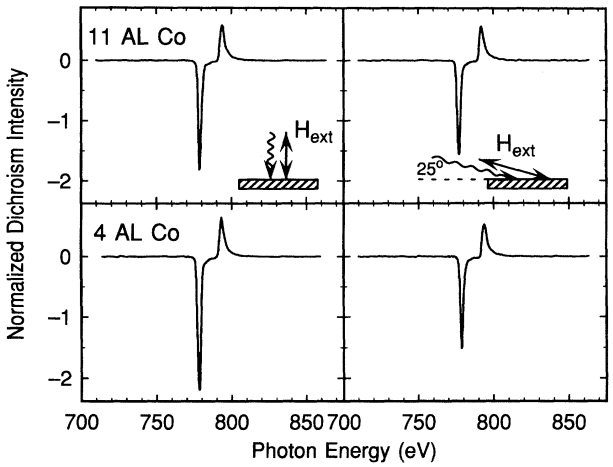

FIG. 1. Normalized x-ray magnetic circular dichroism spectra at the Co L_3(778 eV) and L_2(793 eV) edges for a Au/Co/Au staircase sample and Co thicknesses of 4 and 11 AL. Spectra are shown for normal and grazing x-ray incidence relative to the surface. In each case the 10 kOe magnetic field was parallel to the x-ray incidence direction.

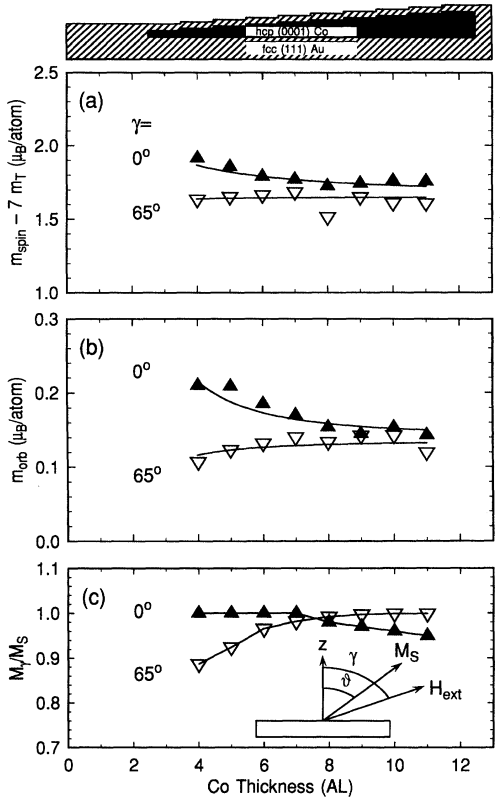

FIG. 2. (a) Moment $m_{\mathrm{spin}} - 7m_T$ derived from the XMCD spectra and Eq. (2) for normal and grazing orientations, respectively. (b) Orbital moment m_{orb} for the same sample orientations derived by use of Eq. (1). (c) Magnetization components M_{γ}/M_S in 10 kOe external field along the field direction γ and angle definitions. The moments plotted in (a) and (b) are already corrected for incomplete saturation at the different thickness steps.

the thickness dependent magnetization component along the field direction $M_\gamma/M_S = \cos(\gamma - \vartheta)$, also plotted in Fig. 2(c). The equilibrium magnetization angle ϑ was determined from polar Kerr hysteresis loops $\theta_K^\gamma(H)$ measured at a field angle γ in fields $\pm H$, according to the relation $\theta_K^\gamma(10\text{ kOe})/\theta_K^{\gamma=0^\circ}(20\text{ kOe}) = \cos\vartheta$. The moments in Figs. 2(a) and 2(b) become increasingly anisotropic toward the thin end of the staircase.

It has been shown recently that the magnetic dipole term in the spin sum rule can be isolated in an angle-dependent XMCD measurement by applying the approximate symmetry relation for $3d$ metals $\langle T_x\rangle + \langle T_y\rangle + \langle T_z\rangle = 0$ [14]. Thus, in the absence of in-plane anisotropies we can write $m_T^\perp + 2m_T^\parallel = 0$ and separately determine the intra-atomic dipole components m_T^γ and the spin moment m_{spin}. The actual in-plane component $m_T^\parallel$ is obtained from the measured components m_T^γ and $m_T^\perp$ according to $m_T^\gamma = m_T^\perp \cos^2\gamma + m_T^\parallel \sin^2\gamma$ [25]. The results of this analysis are plotted in Figs. 3(a) and 3(b). The spin moment itself [Fig. 3(a)] is essentially thickness independent. The anisotropy in the spin density, on the other hand, shows a strong Co thickness dependence as shown in Fig. 3(b). At $t_{\text{Co}} = 4$ AL we find $m_T^\parallel - m_T^\perp = 0.048\mu_B$, relating to sizable corrections of $7m_T^\parallel = 0.112\mu_B$ and $7m_T^\perp = -0.224\mu_B$ in Eq. (2). The data follow a simple $m_{T,S}/t_{\text{Co}}$ dilution law (solid lines) with $m_{T,V} = 0$ [27], leading to large extrapolated corrections $7m_{T,S}^\parallel = 0.43\mu_B$ and $7m_{T,S}^\perp = -0.86\mu_B$ for a single atomic layer of Co sandwiched between Au.

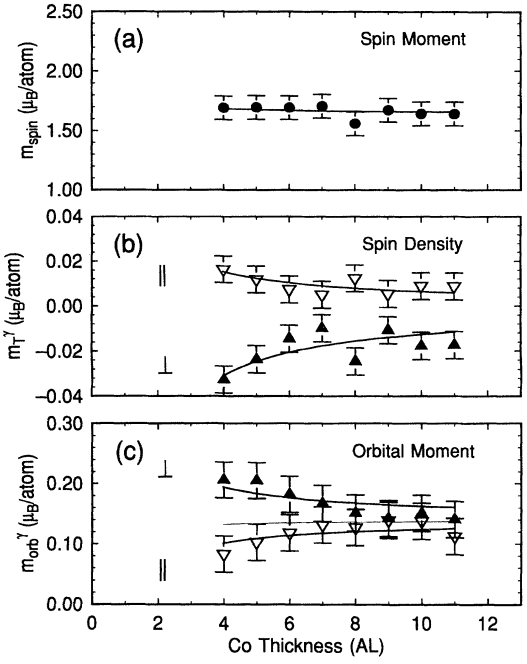

FIG. 3. (a) Spin moment m_{spin} and (b) electron spin density anisotropy $m_T^\perp$ and $m_T^\parallel$ as a function of Co thickness. $m_T^\parallel$ and $m_{\text{orb}}^\parallel$ are the in-plane projected moments calculated from the measured quantities at $\gamma = 65°$ and $\gamma = 0°$, as discussed in the text. The solid lines are fits [27] to the data. (c) Orbital moment $m_{\text{orb}}^\perp$ and $m_{\text{orb}}^\parallel$ as a function of Co thickness. The solid lines are fits [27], and the light solid line represents the angle averaged orbital moment.

We have also determined the in-plane orbital moment $m_{\text{orb}}^\parallel$ [25], which together with $m_{\text{orb}}^\perp$ is replotted in Fig. 3(c). The thickness dependent anisotropy, $\Delta m_{\text{orb}} = m_{\text{orb}}^\perp - m_{\text{orb}}^\parallel$, takes values up to $\approx 0.12\mu_B$ at the 4 AL Co step. Δm_{orb} decays rapidly and becomes smaller than the experimental error for thicknesses larger than 7 AL. A $m_{\text{orb},S}/t_{\text{Co}} + m_{\text{orb},V}$ behavior, again, can be fitted to the data [27]. We extrapolate monolayer orbital moments of $m_{\text{orb},S}^\perp = 0.36\mu_B$ and $m_{\text{orb},S}^\parallel \approx 0\mu_B$ for perpendicular and in-plane orientations, respectively. Here the bulk Co orbital moment was assumed to be $m_{\text{orb},V} = 0.14\mu_B$ for both orientations. The light solid line in Fig. 3(c) represents the angle averaged orbital moment, $(m_{\text{orb}}^\perp + 2m_{\text{orb}}^\parallel)/3$ [25], which is essentially independent of the Co thickness.

Figure 3 shows that the thickness dependence of the anisotropies in m_{orb} and m_T is inversely correlated. At the thin end of the staircase we find $m_{\text{orb}}^\perp > m_{\text{orb}}^\parallel$, while $m_T^\parallel > m_T^\perp$. In a picture based on the symmetry of the d orbitals [14], this indicates that there is a larger contribution to the Co spin moment from the in-plane (d_{xy} and $d_{x^2-y^2}$) than from the out-of-plane orbitals [28]. The perpendicular orbital moment direction also arises from the in-plane orbitals, supporting the intuitive picture that in-plane orbits lead to a perpendicular orbital moment.

Bruno [5] has shown in a perturbation theory treatment that the energy anisotropy in a uniaxial system caused by the spin-orbit interaction $\xi\mathbf{l}\cdot\mathbf{s}$ is directly linked to the anisotropy of the orbital moment, and for a more-than-half filled d shell one obtains

$$\Delta E_{\text{SO}} = -\frac{G}{H}\frac{\xi}{4\mu_B}(m_{\text{orb}}^\perp - m_{\text{orb}}^\parallel), \qquad (3)$$

where the factor G/H depends on the details of the band structure and is estimated to be about 0.2 for Co [29]. Our results show that $m_{\text{orb}}^\perp > m_{\text{orb}}^\parallel$ and the easy axis is therefore perpendicular to the surface (ΔE_{SO} is negative, K_1 is positive [30]). Using the experimentally determined value $\Delta m_{\text{orb}} \approx 0.12\mu_B$ at $t_{\text{Co}} = 4$ AL and $\xi = 0.05$ eV [5], we obtain $\Delta E_{\text{SO}} \approx -3 \times 10^{-4}$ eV/atom with $G/H = 0.2$. The measured anisotropy (volume) density at that thickness is $K_1 = 2.2$ MJ/m^3, or $\Delta E_{\text{SO}} = -1.6 \times 10^{-4}$ eV/atom, assuming a bulk Co atomic density of 8.97×10^{-28} m^{-3}. This is in satisfactory agreement with the estimate according to Eq. (3), and can thus be viewed as direct evidence for the simple perturbation theory model of Bruno [5].

The importance of the present work is that it provides direct experimental proof for a simple picture for the

microscopic origin of the MCA. Below 11 AL of Co, the anisotropy energy associated with the orbital moment exceeds the value of the extra-atomic spin-spin dipole interaction, which favors in-plane orientation of the spin moment ($2\pi M_S^2 = 9 \times 10^{-5}$ eV/atom), and the magnetization turns into the perpendicular direction favored by the orbital moment. Because the spin-orbit coupling energy ($\sim 10^{-2}$ eV/atom) is large compared to the anisotropy energies associated with the spin and orbital moments ($\sim 2 \times 10^{-4}$ eV/atom), the two moments remain coupled (parallel), and we have the interesting situation that the small orbital moment redirects the larger spin moment into a perpendicular alignment (easy axis).

This work was carried out in part at SSRL, which is operated by the Department of Energy, Division of Chemical Sciences. We thank Patrick Bruno for valuable discussions. R. N. wishes to acknowledge support by the Stanford Center for Materials Research through National Science Foundation Grant No. DMR-9400372. A. C. would like to thank the Alexander von Humboldt foundation for continuous support.

*Present address: Universtät-GH-Duisburg, 47048 Duisburg, Germany.

[1] J. Kanamori, in *Magnetism,* edited by G. T. Rado and H. Suhl (Academic, New York, 1963), Vol. I.

[2] L. Néel, J. Phys. Radium **15**, 225 (1954).

[3] G. H. O. Daalderop, P. J. Kelly, and M. F. H. Schuurmans, Phys. Rev. B **41**, 11 919 (1990).

[4] U. Gradmann and J. Müller, Phys. Status Solidi **27**, 313 (1968); U. Gradmann, Appl. Phys. **3**, 161 (1974); P. F. Carcia, A. D. Meinholdt, and A. Suna, Appl. Phys. Lett. **47**, 178 (1985); F. J. A. den Broeder,W. Hoving, and P. J. H. Bloemen, J. Magn. Magn. Mater. **93**, 562 (1991).

[5] P. Bruno, Phys. Rev. B **39**, 865 (1989); P. Bruno, in *Physical Origins and Theoretical Models of Magnetic Anisotropy* (Ferienkurse des Forschungszentrums Jülich, Jülich, 1993).

[6] U. Gradmann, in *Ferromagnetic Materials,* edited by K. H. J. Buschow (Elsevier, Amsterdam, 1993), Vol. 7.

[7] J. G. Gay and R. Richter, Phys. Rev. Lett. **56**, 2728 (1986).

[8] G. Y. Guo, W. M. Temmerman, and H. Ebert, J. Phys. Condens. Matter **3**, 8205 (1991).

[9] G. H. O. Daalderop, P. J. Kelly, and F. J. A. den Broeder, Phys. Rev. Lett. **68**, 682 (1992).

[10] K. Kyuno, R. Yamamoto, and S. Asano, J. Phys. Soc. Jpn. **61**, 2099 (1992).

[11] D. Wang, R. Wu, and A. J. Freeman, Phys. Rev. Lett. **70**, 869 (1993).

[12] R. H. Victora and J. M. MacLaren, Phys. Rev. B **47**, 11 583 (1993).

[13] M. Cinal, D. M. Edwards, and J. Mathon, Phys. Rev. B **50**, 3754 (1994).

[14] J. Stöhr and H. König, preceding Letter, Phys. Rev. Lett. **75**, 3748 (1995).

[15] Although enhancements of orbital moments have been observed before [Ref. [16] and G. van der Laan *et al.,* Phys. Rev. Lett. **69**, 3827 (1992)], their anisotropy has never been measured.

[16] Y. Wu, J. Stöhr, B. D. Hermsmeier, M. G. Samant, and D. Weller, Phys. Rev. Lett. **69**, 2307 (1992).

[17] D. Weller, Y. Wu, J. Stöhr, M. G. Samant, B. D. Hermsmeier, and C. Chappert, Phys. Rev. B **49**, 12 888 (1994).

[18] For details see D. Renard and G. Nihoul, Philos. Mag. B **55**, 75 (1987); C. Cesari *et al.,* J. Magn. Magn. Mater. **78**, 296 (1989); J. Ferré *et al.,* Appl. Phys. Lett. **56**, 1588 (1990); V. Grolier *et al.,* Phys. Rev. Lett. **71**, 3023 (1993).

[19] t^* was determined from the equation $2K_S = t^*(2\pi M_S^2 - K_V - K_2)$. See, e.g., P. Beauvillain *et al.,* J. Appl. Phys. **76**, 6078 (1994).

[20] B. T. Thole, P. Carra, F. Sette, and G. van der Laan, Phys. Rev. Lett. **68**, 1943 (1992).

[21] P. Carra, B. T. Thole, M. Altarelli, and X. Wang, Phys. Rev. Lett. **70**, 694 (1993).

[22] R. Wu, D. Wang, and A. J. Freeman, Phys. Rev. Lett. **71**, 3581 (1993).

[23] R. Wu and A. J. Freeman, Phys. Rev. Lett. **73**, 1994 (1994).

[24] M. G. Samant *et al.,* Phys. Rev. Lett. **72**, 1112 (1994).

[25] For a uniaxial system we assume m_{orb} and m_T in Eqs. (1) and (2) to vary as (to lowest order) $m^\gamma = m_0 - \Delta m \sin^2\gamma$. This can be rewritten as $m^\gamma = m^\perp \cos^2\gamma + m^\parallel \sin^2\gamma$, used here to calculate the in-plane moments ($\gamma = 90°$). The angle averaged moment is given by $(1/4\pi)\int m_{\mathrm{orb}}^\gamma \, d\Omega = (m^\perp + 2m^\parallel)/3$.

[26] O. Eriksson, B. Johansson, R. C. Albers, A. M. Boring, and M. S. S. Brooks, Phys. Rev. B **42**, 2707 (1990); P. Söderlind, O. Eriksson, B. Johansson, R. C. Albers, and A. M. Boring, Phys. Rev. B **45**, 12 911 (1992).

[27] The moments derived by XMCD are average moments over the probed Co volume and are determined by the actual moment profile $m(z)$, the Co film thickness t, and the mean electron yield sampling depth λ in Co, according to $\overline{m(t)} = \int_0^t m(z)e^{-z/\lambda}\,dz / \int_0^t e^{-z/\lambda}\,dz$. For the fits in Fig. 3 we assumed moments m_S for the two interfacial Co layers, m_V for all interior layers, and $\lambda = 12.5$ AL, as determined independently. The so-obtained fits give almost identical results as a simple dilution law, $m_S/t + m_V$, which is obtained for $\lambda \gg t$.

[28] G. H. O. Daalderop, P. J. Kelly, and M. F. H. Schuurmans, Phys. Rev. B **50**, 9989 (1994). Note, however, that here the electron spin density for a Co monolayer is predicted to be preferentially out of plane, opposite to the present results for Au/Co/Au.

[29] P. Bruno (private communication). $G/H = 1$ represents the case that the exchange splitting Δ_{ex} is much larger than the bandwidth W. For a transition metal, however, the condition $\Delta_{ex} \gg W$ is not fulfilled and G/H becomes smaller than 1. A rough estimate yields $G/H \approx 1/5$ or smaller.

[30] Note that $\Delta E_{\mathrm{SO}} = E_{\mathrm{SO}}^\perp - E_{\mathrm{SO}}^\parallel = -K_1$ with the convention $E_{\mathrm{SO}} = K_0 + K_1 \sin^2\theta$ used in Ref. [5].